ANALYSIS OF PERTURBATIONS AND STATION-KEEPING REQUIREMENTS IN HIGHLY-INCLINED GEOSYNCHRONOUS ORBITS

Elena Fantino[1], Roberto Flores[2], Alessio Di Salvo[3], and Marilena Di Carlo[4]

[1]*Space Studies Institute of Catalonia (IEEC), Polytechnic University of Catalonia (UPC), E.T.S.E.I.A.T., Colom 11, 08222 Terrassa (Spain), elena.fantino@upc.edu*

[2]*International Center for Numerical Methods in Engineering (CIMNE), Polytechnic University of Catalonia (UPC), Building C1, Campus Norte, UPC, Gran Capitán, s/n, 08034 Barcelona (Spain)*

[3]*NEXT Ingegneria dei Sistemi S.p.A., Space Innovation System Unit, Via A. Noale 345/b, 00155 Roma (Italy), alessio.disalvo@next.it*

[4]*Department of Mechanical and Aerospace Engineering, University of Strathclyde, 75 Montrose Street, Glasgow G1 1XJ (United Kingdom), marilena.di-carlo@strath.ac.uk*

Abstract: *There is a demand for communications services at high latitudes that is not well served by conventional geostationary satellites. Alternatives using low-altitude orbits require too large constellations. Other options are the Molniya and Tundra families (critically-inclined, eccentric orbits with the apogee at high latitudes). In this work we have considered derivatives of the Tundra type with different inclinations and eccentricities. By means of a high-precision model of the terrestrial gravity field and the most relevant environmental perturbations, we have studied the evolution of these orbits during a period of two years. The effects of the different perturbations on the constellation ground track (which is more important for coverage than the orbital elements themselves) have been identified. We show that, in order to maintain the ground track unchanged, the most important parameters are the orbital period and the argument of the perigee. Very subtle changes in the orbital period (due mainly to lunar perturbations) cause a large east-west drift of the ground trace which dwarfs the displacement due to the regression of the ascending node. From these findings, a station-keeping strategy that minimizes propellant consumption has then been devised. Our results offer interesting guidelines for the design and operation of satellite constellations using these orbits.*

Keywords: *Orbits, Geosynchronous, Perturbations, Station-Keeping, Communications.*

1. Introduction

The objective of this contribution is to analyse specific orbital solutions in response to the growing interest towards the extension of satellite telecommunications coverage to geographical regions at high latitude, say beyond 55°. Geostationary links work well at low and mid latitudes, with the coverage progressively degrading, for example, when moving northwards through Alaska and the Canadian territories in America, or the Arctic in Europe. Bringing satellite communications to the high latitudes is beneficial not only to land users (television and radio signals, voice and data transmission), but also to aircraft on polar routes, to maritime connections and in view of UAV applications. Low-Earth Orbit (LEO) constellations ensure global coverage provided they include many satellites (66 in the case of Iridium [1]). Other possibilities are the so-called responsive orbits evaluated by [2], and subdivided into five types: Cobra, Magic, LEO Sun-Synchronous, LEO Fast Access, LEO Repeat Coverage, with periods ranging from typical LEO values (1.5-2 hours) to 8 hours (Cobra orbit) and requiring a few to several satellites operating in different orbital planes.

[3] describes the Wonder orbit, a low-altitude, highly elliptical orbit with critical inclination and designed to provide a non-drifting repeating ground track. With the aim at providing coverage at high latitudes (60°N) with minimum elevations of 35°, a constellation of ten satellites in two planes, with orbital period of 3.4 hours and perigee height of 600km is suggested. [4] provides an examination of the orbital evolution and lifetime of the Russian Molniya satellites which occupy low-perigee, semi-synchronous orbits at critical inclination. The influence of the several perturbing factors on the long-term orbital evolution is found to be related to the choice of the initial value of the right ascension of the ascending node and the argument of perigee. [5] studies a constellation of satellites in Tundra orbits (i.e., geosynchronous, eccentric and critically inclined) and analyses in detail the effect of each perturbation (Earth's aspheric potential, solar and lunar gravity, solar radiation pressure, atmospheric drag) on the orbital elements. Frozen orbital elements are identified using a double-averaged potential function for the third-body perturbation. This reduces station-keeping costs as far as the eccentricity and argument of perigee are concerned. The maneuver strategy consists in a bang-bang control method. [6] presents the orbital evolution and station-keeping corrections for a geosynchronous polar orbit, called Tundra Polar due to its similarities with the traditional Tundra orbit in terms of orbital period and eccentricity. The orbit is thought to serve mission objectives such as weather monitoring and forecasting for the North Pole and Canada. The physical model consists in a 12×12 gravity field, solar and lunar gravity and solar radiation pressure perturbations. Thanks to its 90° inclination, the Tundra Polar orbit is not affected by the drift of the ascending node due to the second terrestrial zonal harmonic. The orbital parameters are selected so as to limit the variation of right ascension of the ascending node and inclination. In this way, only in-plane maneuvers for eccentricity and argument of perigee correction must be implemented. The work of [7] offers an extended analysis of satellite constellations alternatives for the Arctic communications system. A total of 15 solutions are considered, consisting in inclined, eccentric orbits with periods of 12, 16, 18 and 24 hours respectively. The assessment is carried out by analysing coverage, elevation, azimuth, launch cost, radiation exposure and station-keeping requirements. The physical model accounts for the Earth's gravitational potential developed to the second zonal harmonic and an estimation of the effects of the luni-solar third-body perturbation. The study identifies the best solution as that consisting in three satellites in three equally-spaced orbital planes and characterized by a 12 hours period.

Communications service to high-latitude regions is currently being provided by the Sirius constellation of digital radio satellites[1] in the continental United States and Canada (Fig. 1). Satellites Radiosat 1 through Radiosat 3 fly in geosynchronous highly-elliptical orbit in a 23 hours, 56 minutes orbital period (one sidereal day). The elliptical path of this satellite constellation ensures that each satellite spends about 16 hours a day over the continental United States, with at least one satellite over the country at all times. The inclinations range from 60° to 65°, approximately. The advantage of a geosynchronous inclined orbit is that its period is equal to that of the Earth's rotation (repetition of orbital pattern), which gives the ground trace a characteristic figure-eight pattern centered at the chosen reference longitude. Furthermore, if the orbit is eccentric and the perigee is placed at the point of lowest latitude, the apogee dwell occurs over the northern hemisphere and allows long

[1] http://www.celestrak.com/cgi-bin/TLE.pl?CATNR=26390 for Sirius-1; http://www.celestrak.com/cgi-bin/TLE.pl?CATNR=26483 for Sirius-2; http://www.celestrak.com/cgi-bin/TLE.pl?CATNR=26626 for Sirius-3; checked on 27/09/2015

contacts per orbit of the same satellite with the users. Full coverage is obtained by using three satellites on equally-spaced orbital planes (i.e, at 120° separation, see Fig. 1). In this contribution, we have explored a family of geosynchronous, inclined, eccentric orbits with orbital elements chosen so as to ensure service in the regions affected by low GEO coverage. We have simulated the evolution of these orbits over an appropriate time interval and using a force model whose degree of approximation is set at any moment by the desired accuracy level. Eventually, we have thought of an optimal maneuver strategy in order to maintain the ground tracks, and we have estimated the amount of fuel required for its application. Section 2. introduces the physical model. Sect. 3. illustrates the characteristics of the adopted orbital family and the simulations setup. The orbital evolution of the several orbits is discussed in Sect. 4., whereas the station-keeping strategy and the result of its application are explained in Sect. 5. The conclusions are drawn in Sect. 6.

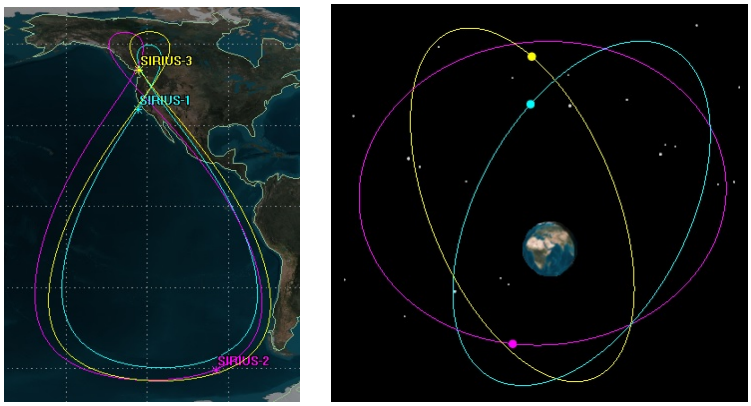

Figure 1. The Sirius constellation: ground track (left) and three-dimensional view of the orbits (right).

2. The physical model

The physical model accounts for the gravitational acceleration $\mathbf{a}_E$ due to the Earth, the accelerations $\mathbf{a}_M$ and $\mathbf{a}_S$ caused by the third-body perturbations of Moon and Sun, respectively, the perturbation $\mathbf{a}_{SRP}$ due to the solar radiation pressure and the term $\mathbf{a}_R$ associated to the relativistic correction to gravity. In other words, the acceleration $\mathbf{a}$ of the satellite is

$$\mathbf{a} = \mathbf{a}_E + \mathbf{a}_M + \mathbf{a}_S + \mathbf{a}_{SRP} + \mathbf{a}_R. \tag{1}$$

The effect of atmospheric drag on the orbit has not been taken into account given the very high perigees (radial distances $> 2.5 \cdot 10^4$ km, see Sect. 3.) of the orbits considered.

2.1. Earth's gravitational potential

The traditional approach for representing the gravitational potential V at a point P in outer space is based on a spherical harmonic expansion in Associated Legendre Functions (ALFs) [8]

$$V(r,\phi,\lambda) = \frac{GM_E}{r} \sum_{n=0}^{N} \left(\frac{R_E}{r}\right)^n \sum_{m=0}^{n} P_n^m(\sin\phi)\left(C_{nm}\cos m\lambda + S_{nm}\sin m\lambda\right), \tag{2}$$

where r, ϕ and λ are the Earth-centered spherical equatorial coordinates of P (respectively, radial distance, latitude and longitude from the fundamental meridian), R_E is the mean Earth's radius, GM_E is the Earth's gravitational parameter (the product of the Universal gravitational constant and the mass of the Earth), the quantities C_{nm} and S_{nm} are the Stokes coefficients and, finally, $P_n^m(\sin\phi)$ is the ALF of the first kind of degree n and order m. In Eq. 2, truncation of the series is applied at a maximum degree N (hereinafter called expansion degree). Eventually,

$$\mathbf{a}_E = \nabla V. \tag{3}$$

Unfortunately, the latitudinal derivative of V is singular at $\phi = \pm 90^\circ$, a drawback when dealing with polar orbits.

In this work, the harmonic synthesis of the geopotential and its first-order gradient is carried out in Cartesian Earth-fixed coordinates and using Helmholtz polynomials H_n^m [9, 10]. The method is due to [11] and is singularity-free. The version here adopted is that described in [12]: it incorporates improved recursion schemes on the Helmholtz polynomials and deals with the sums by accumulating so-called lumped coefficients (harmonic sums over the degree), which yields better performances. The expression for the geopotential $V(P)$ is

$$V(P) = \sum_{m=0}^{N} (A_m \cos m\lambda + B_m \sin m\lambda) \cos^m \phi, \tag{4}$$

in which

$$A_m = \sum_{n=m}^{N} \rho_n C_{nm} H_n^m \tag{5}$$

$$B_m = \sum_{n=m}^{N} \rho_n S_{nm} H_n^m, \tag{6}$$

$\rho_n = (GM_E/r)(R_E/r)^n$ being a parallactic factor. Formulas for the derivatives of V (i.e., the cartesian components of the accelerations) and more details on the computation of the polynomials can be found in [12, 13, 14]. Thus, with the issue of the singularity at the poles solved, the computation of quasi-polar or polar orbits can be carried out without loss of precision.

The adopted gravitational field is the Earth Gravitational Model EGM2008 [15] in its zero-tide version. It provides the fully-normalized, unit-less, Stokes coefficients and their associated error standard deviations. The model is complete to degree and order 2159; however, for the reasons exposed in Sect. 3., it has been truncated to degree and order 40 for use in our software.

2.2. Third-body perturbations

The gravitational attraction of either the Sun or the Moon on the spacecraft is responsible for an acceleration $\mathbf{a}_{3B}$ which can be expressed as follows (see [16]):

$$\mathbf{a}_{3B} = -GM_B \left[\frac{\mathbf{r}_{s/c} - \mathbf{r}_B}{|\,\mathbf{r}_{s/c} - \mathbf{r}_B\,|^3} + \frac{\mathbf{r}_B}{r_B^3} \right], \tag{7}$$

where M_B is the mass of the perturbing body (i.e., the Sun or the Moon), $\mathbf{r}_{s/c}$ is the geocentric position of the spacecraft and $\mathbf{r}_B$ is the geocentric position of the perturbing body. Evaluation of Eq. 7 requires knowledge of the geocentric position of the Sun and the Moon. Since the forces that these two bodies exert on the spacecraft are much smaller than the attraction of the Earth, it is not necessary to determine their coordinates to the highest precision when calculating the perturbing acceleration acting on the satellite. Approximate positions accurate to about 0.1-1% are sufficient. Eventually, Eq. 7 is particularized for the case of the Moon and the Sun, yielding the corresponding accelerations $\mathbf{a}_M$ and $\mathbf{a}_S$.

2.2.1. Approximate position of the Sun

The geocentric position vector of the Sun is determined from the heliocentric position vector of the Earth-Moon barycenter. The reference frame is the mean ecliptic and equinox of J2000. The model is an approximate one, consisting in propagating the Keplerian elements according to given constant rates, then transforming the orbital position (perifocal coordinates) to the heliocentric ecliptic reference frame and eventually to the equatorial one. Details, data and formulas are available at the Solar System Dynamics website[2].

2.2.2. Approximate position of the Moon

Simulation of the orbital motion of the Moon is carried out by assuming a set of mean orbital elements with respect to the mean ecliptic and equinox of J2000 and taking into account the linear regression of the ascending node and the linear precession of the line of apsides. This is followed by rotations to ecliptic and eventually to equatorial coordinates. The mean orbital elements and the rates of the two angular quantities are publicly available through the Solar System Dynamics website[2].

2.3. Solar radiation pressure

As for the interactions of the spacecraft surface with the solar radiation, we have assumed a spherical shape with rectangular wing-like solar panels We have adopted a simplified expression for the corresponding acceleration, a_{SRP}, valid when the surface normal points in the direction of the Sun [16]:

$$\mathbf{a}_{SRP} = -f\left(\frac{P_S}{4\pi d_S^2 c}\right)\left(\frac{A}{m}\right)(1+k)\mathbf{u}_S. \tag{8}$$

$P_S = 3.846 \cdot 10^{26}$ W is the luminosity the Sun, d_S is the Sun-spacecraft distance, c is the speed of light in vacuum, A/m is the front area-to-mass ratio of the satellite, k is the surface reflectivity (ranging from 0 for complete absorption to 1 for specular reflection) and $\mathbf{u}_S$ is the satellite-to-Sun unit vector.

The symbol f represents the shadow factor, computed according to the double-cone model for solar

[2]http://ssd.jpl.nasa.gov/, checked on 27/09/2015

eclipses [16]:

$$f = \begin{cases} 0: & \text{satellite in umbra} \\ 1: & \text{satellite in sunlight} \\ > 0 \text{ and } < 1: & \text{satellite in penumbra} \end{cases} \tag{9}$$

For standard communication satellites the A/m ratio is about $0.01\text{m}^2/\text{kg}$, yielding accelerations below 10^{-7}m/s^2.

2.4. Relativistic correction

The effects of General Relativity can be included by adding a perturbation δV to the Newtonian gravity potential with the form:

$$\delta V = -\frac{GM_E L^2}{c^2 r_{s/c}^3}, \tag{10}$$

where L denotes the spacecraft's specific angular momentum. For the orbits under study the characteristic magnitude of the relativistic correction is 10^{-10}m/s^2.

3. Simulations setup

3.1. Selection of the orbits

We have considered a set of orbits derived from the traditional Tundra. They are geosynchronous, hence their orbital mean motion n_0 is equal to $7.292 \cdot 10^{-5}$rad/s (i.e., the value of the Earth's sidereal rotation rate), hence the orbital period T_0 equals 86165.5s. Furthermore, these orbits are inclined and eccentric. In order to provide service to high-latitude users, the perigee is positioned at the point of lowest latitude, corresponding to an argument of perigee ω_0 of 270°. Figure 2 illustrates the world population distribution in latitude and longitude: in the northern hemisphere the most populated regions are centered around 100°W (North America), 10°E (Europe) and 100°E (between Russia and China). These longitudes have been chosen as the most economically sensible for operation of a constellation of communication satellites.

The values of eccentricity e_0 and inclination i_0 have been selected in order to obtain a satisfactory coverage of the areas of interest. Following the requirement on the Sirius satellites, we have set the minimum elevation over the horizon at 60° for communications operations. By tracking the three satellites of the constellation along their orbits, we have mapped the points on the Earth's surface at which the visibility requirement is satisfied by at least one satellite at all times. Examples of such maps are illustrated in Fig. 3. Upon trying different combinations of e_0 and i_0, we have identified the values which satisfy the constraint and maximise the coverage over the area of interest. The plot of population distribution shows the scarcity of population above 55°N latitude, with an extremely small percentage of people living in areas beyond 65°N. Therefore, coverage in areas above 65°N has not been considered as it is not economically justifiable. Moreover, special applications like maritime, aircraft and UAV navigation can be served without the requirement for high elevation angles (tall obstacles blocking the view of the sky are very scarce in the Artic region).

The critical inclination has been included in the set for the sake of completeness and to compare the

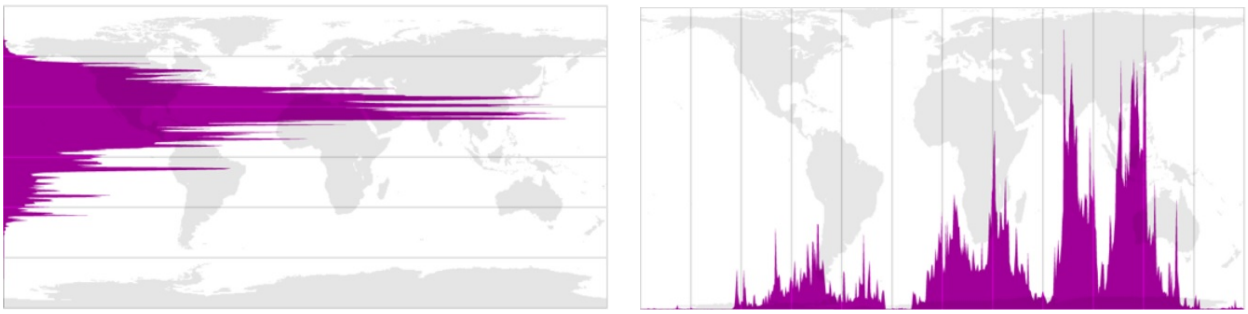

Figure 2. Distribution of world population by latitude (left) and by longitude (right), respectively, as of 2000. Data from http://www.radicalcartography.net/, checked on 27/09/2015

Table 1. Selected combinations of initial eccentricities e_0 and inclinations i_0 (in degrees).

Set	1	2	3	4	5	6	7	8	9
e_0	0.25	0.25	0.30	0.25	0.30	0.35	0.40	0.35	0.40
i_0	55.0	60.0	60.0	63.4	63.4	63.4	63.4	70.0	70.0

evolution of the classical Tundra with the rest of geosynchronous inclined orbits. To each of the nine combinations of e_0 and i_0, we have assigned five equally-spaced values for the right ascension of the ascending node Ω_0, namely 0°, 60°, 120°, 180° and 240°. This results into 45 sets of initial orbital elements. The satellite is assumed to be at perigee when the simulations start (true anomaly $\theta_0 = 0°$).

3.2. Choice of the integration accuracy

The choice of the perturbations to model depends on the level of accuracy sought. For Tundra-like orbits, it has been decided that station-keeping to within 1° accuracy is sufficient for the intended applications. As a matter of fact, a satellite angular displacement of 1° corresponds roughly to a change of 100km in the ground trace. This is a small distance compared with the size of the coverage area (typically several thousand kilometers). In the present study, the station-keeping requirements over two years are studied. This is twice the period of the slowest varying cyclic perturbation (solar) and is thus considered representative of the long-term evolution. To be able to sense 1° errors in position after two years, the discretization error introduced by the orbit propagator must be small compared with this value. A uniform drift of 1° over two years is equivalent to $1.4 \cdot 10^{-3}$degrees per orbit. Given the altitude of the orbits under study, this corresponds to more than 400km per orbit. Therefore, the error in the trajectory propagation must be at least 10 times smaller, i.e., 40km/orbit. The propagator tolerance and time step must be chosen so as to respect the target accuracy. It has been determined through numerical experiments that using a relative tolerance of 10^{-6} and a maximum time step of 600s produces errors well below the required 40 km / orbit threshold. The required accuracy also determines the magnitude of the perturbing forces to consider. A constant acceleration of 10^{-8}m/s^2 acting for one day (the orbital period) causes a drift of 40km. This means that perturbing accelerations below such value can be neglected without altering the quality of the results. Note also that most perturbations are likely to fluctuate instead of being uniform, so their cumulative effect will be smaller (this is a worst case scenario estimate). According to this criterion, the perturbations due to atmospheric drag and relativistic corrections

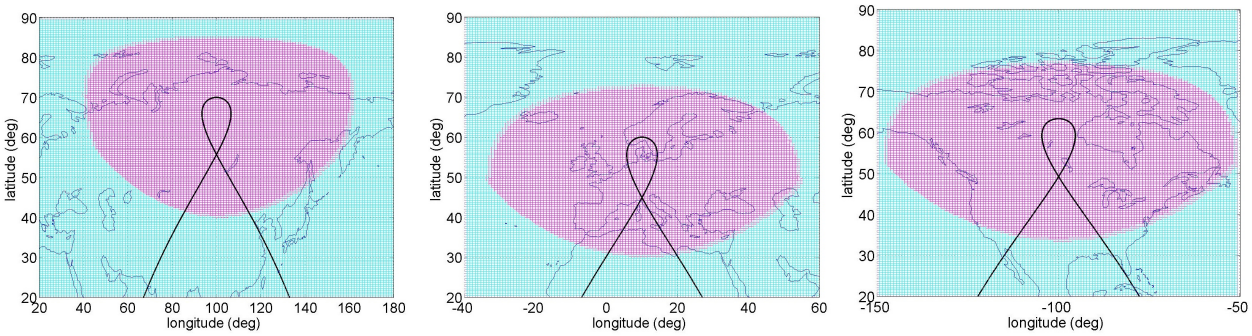

$(e_0, i_0) = (0.40, 70^\circ)$ $(e_0, i_0) = (0.25, 60^\circ)$ $(e_0, i_0) = (0.30, 63.4^\circ)$

Figure 3. Coverage from three orbits at the three selected reference values of the longitude, i.e., 100°E, 10°E, 100°W.

can be ignored as the fall well below the 10^{-8}m/s^2 level. The effect of solar radiation pressure is barely appreciable and has a marginal effect in the station-keeping requirements.

3.3. Choice of the expansion degree of the Earth's gravitational acceleration

When performing the harmonic synthesis of the geopotential and its first-order gradient, the number of spherical harmonics to retain (i.e., the expansion degree) is determined by the accuracy requirement. Given that higher order harmonics decay rapidly with altitude, the expansion degree necessary to meet the target accuracy decreases with height. To make the computations as efficient as possible, the number of degrees to retain must be determined dynamically while the trajectory is being computed. To determine the optimum expansion degree at each altitude a sample of 36 longitudes and 17 latitudes has been analyzed (corresponding to points spaced 10° along a sphere). The expansion degree required to reduce the truncation error below 10^{-8}m/s^2 at each point of the grid has been determined (i.e., the degree for which the difference between the complete EGM2008 model and the truncated series is less than the threshold acceleration). This procedure has been repeated for several altitudes (in 2000 km steps) to cover the complete trajectory envelope. The table containing the required expansion degree as a function of altitude is used by the numerical integrator to compute the gravitational acceleration, guaranteeing the required accuracy while keeping the computational cost to a minimum.

4. Orbital evolution

The physical model illustrated in Sect. 2. has been implemented in a numerical code, called CHEOPs (Cartesian Harmonic synthEsis Orbit Propagator). CHEOPs incorporates a 7(8) Runge-Kutta-Fehlberg numerical integrator. The 45 sets of initial conditions presented in Sect. 3.1. have been propagated over intervals of two years, to encompass all the periodicities present in the model. Before the propagation starts, the orbital period is modified in order to remove the linear effect of J_2 on the ground track. Typical values for the resulting correction are of the order of 1s. Due to the high altitudes of these orbits, the expansion degree that the code automatically selects for the simulations never exceeds 3. Figure 4 reports the evolution of the orbital parameters of the subset of orbits characterized by $e_0 = 0.3$ and $i_0 = 60^\circ$ with each of the five values of the initial right

ascension of the ascending node, i.e., $\Omega_0 = 0^\circ$, 60°, 120°, 180°, 240°. The most important secular perturbation is due to the Moon, which causes variations of the orbital period which in turn move the ground track in the East-West direction. The displacement can reach hundreds of degrees over a two-year span and need a major axis correction in order to keep the ground track fixed. On the other hand, the fluctuations of eccentricity and inclination have a very limited effect on the ground track and do not require correction over a two-year period. The maximum drift of the argument of perigee observed is around 20° over two years and needs to be periodically corrected.

5. Station-keeping strategy

5.1. Correction of the argument of perigee drift

We propose two alternative strategies to counteract the drift of the line of apsides, one based on impulsive maneuvers and one applying continuous low thrust.

5.2. Impulsive maneuver

To carry out an in-plane rotation of the major axis of the orbit, an optimized impulsive two-burn maneuver has been used. It uses a transfer elliptical orbit with the major axis oriented halfway between the initial and the final orbits. Due to the symmetry of the problem, the two burns have the same magnitude. The transfer orbit has two degrees of freedom, i.e., the eccentricity e and the true anomaly θ of the initial burn. The optimum combination has been found with a two-pass algorithm. For each candidate value of θ, the value of e yielding the minimum impulse is found by solving numerically the equation $\partial \Delta v(e,\theta)/\partial e = 0$. This is easily accomplished because the partial derivative has a simple expression. Next, the optimum true anomaly is found using a minimization algorithm which does not require gradients (Brent's method).

5.3. Continuous low-thrust maneuver

The correction of the argument of perigee can be performed using an electrical engine. Let the components of the acceleration $\mathbf{a}_T$ imparted by the low-thrust engine be denoted a_{T1}, a_{T2} and a_{T3} in a radial-transverse-normal reference frame. It is possible to change ω while keeping the semimajor axis a and the eccentricity e constant, by applying the following in-plane acceleration over thrust arcs centered at perigee [17]:

$$\begin{cases} a_{T1} = a_T \dfrac{\cos E - e}{1 - e\cos E} \\ a_{T2} = -a_T \dfrac{\sqrt{1-e^2}\sin E}{1 - e\cos E} \\ a_{T3} = 0 \end{cases} \tag{11}$$

E is the eccentric anomaly. For a given $\Delta\omega$ to be achieved, the length of the propelled arc is optimized with respect to fuel consumption.

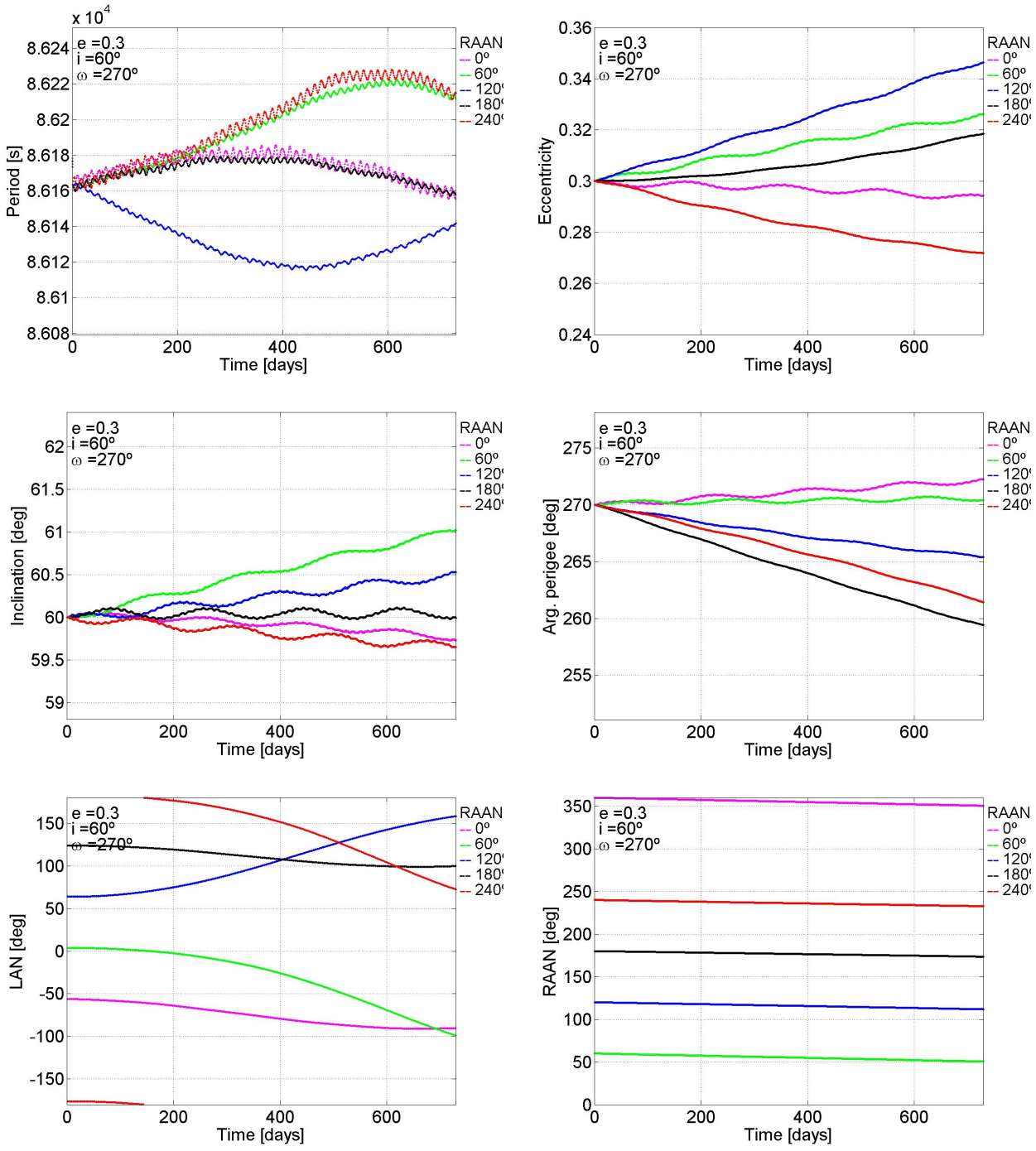

Figure 4. Orbital evolution of a subset of orbits characterized by $e_0 = 0.3$ and $i_0 = 60^\circ$ and all the five values of the initial right ascension of the ascending node, as indicated in the legends. From top left to bottom right the several panels show the behavior of orbital period, eccentricity, inclination, argument of perigee, longitude of the ascending node and right ascension of the ascending node, respectively.

5.4. Correction of the longitude of the ascending node (LAN)

It is important to realize that from the point of view of operation, the position of the orbital plane is of minor importance compared with the correct placement of the ground track. The orbital perturbations cause the right ascension of the ascending node to change and therefore affect the east-west position of the ground track. However, this effect is really minor compared with the changes caused by fluctuations of the orbital period. If the orbital period were to change by δT for any reason, this would cause a drift δLAN of the longitude of the ascending node of $\delta\text{LAN} = -360\delta T/T_0$ degrees per orbit. The magnitude of this drift is so important that it overshadows the effect of the orbital plane precession. Therefore the station-keeping strategy must focus in adjusting the orbital period so as to keep the ground track in place. Any east-west drift of the ground track caused by the different perturbations is countered by introducing an appropriate change in orbital period. This is achieved with a two-burn maneuver which changes the semi-major axis while keeping the other orbital elements unchanged. The first burn takes place at the perigee of the initial orbit and the second at the apogee of the final orbit. Due to the smallness of the change in period required (a few seconds at most) the magnitude of the impulse required can be linearized with respect to the change in period obtaining a very simple closed analytical expression for the propellant expense.

5.5. Estimation of station-keeping cost

The worst-case scenario for the above three maneuvers corresponds to velocity variations Δv of 220m/s, 260m/s and 1m/s over two years, respectively in the case of impulsive perigee drift correction, low-thrust perigee correction and impulsive LAN adjustment. Assuming a spacecraft dry mass of 3000kg and specific impulses of 3400s and 300s for the two types of engine, the Δv budget translates into propellant costs of 230kg and 23kg, respectively.

6. Conclusions

The propellant consumption required to maintain the longitude of the ascending node of the selected orbits is negligible, whereas the cost to keep the perigee fixed is moderate. The difference between low- and high-thrust strategy deserves further investigation. It would be interesting to compare the difference in the mass consumption (which favors the low-thrust solution) with the mass of the propulsion system in order to identify the more convenient option.

Acknowledgements

The authors are grateful to B. Padovan and M. Khun (Curtin University) for advice about the uses of EGM96 and EGM2008.

7. References

[1] Fossa, C. E., Raines, R., Gunsch, G., and Temple, M. “An overview of the IRIDIUM (R) low Earth orbit (LEO) satellite system.” Proceedings of the IEEE 1998 National Aerospace and Electronics Conference, NAECON, pp. 152–159. 1998.

[2] Wertz, J. "Coverage, Responsiveness, and Accessibility for Various "Responsive Orbits"." Proceedings of the 3rd Responsive Space Conference. Los Angeles, CA, 2005.

[3] Cavallaro, G., Phan-Minh, D., and Bousquet, M. "HEO Constellation Design for Tactical Communications." First AESS European Conference on Satellite Telecommunications (ESTEL). Rome, Italy, 2012.

[4] Kolyuka, Y., Ivanov, N., Afanasieva, T., and Gridchina, T. "Examination of the lifetime, evolution and re-entry features for the "Molniya" type orbits." Proceedings of the 21st International Symposium on Space Flight Dynamics — 21st ISSFD. Toulouse, France, 2009.

[5] Bruno, M. and Pernicka, H. "Tundra constellation design and stationkeeping." Journal of Spacecraft and Rockets, Vol. 42, No. 5, pp. 902–912, 2005.

[6] Boccia, V., Grassi, M., Marcozzi, M., Notarantonio, A., and Sollazzo, L. "Mission Analysis and Orbit Control Strategy for a Space Mission on a Polar Tundra Orbit." Proceedings of the 63rd International Astronautical Congress. Naples, Italy, 2012. IAC-12-C1.4.7.

[7] Loge, L. Arctic Communications System Utilizing Satellites in Highly Elliptical Orbits. Ph.D. thesis, Norwegian University of Science and Technology, 2013.

[8] Heiskanen, W. and Moritz, H. Physical Geodesy. Freeman, San Francisco, 1967.

[9] Balmino, G., Barriot, J.-P., and Valés, N. "Non-singular formulation of the gravity vector and gravity gradient tensor in spherical harmonics." Manuscripta Geodetica, Vol. 15, No. 1, pp. 11–16, 1990.

[10] Balmino, G., Barriot, J.-P., Koop, R., Middel, B., and Thong, M., N.C. Vermeer. "Simulation of gravity gradients: a comparison study." Bulletin Géodesique, Vol. 66, No. 3, pp. 261–271, 1991.

[11] Pines, S. "Uniform representation of the gravitational potential and its derivatives." AIAA Journal, Vol. 11, pp. 1508–1511, 1973.

[12] Fantino, E. and Casotto, S. "Methods of harmonic synthesis for global geopotential models and their first-, second- and third-order gradients." Journal of Geodesy, Vol. 83, pp. 595–619, 2009.

[13] Casotto, S. and Fantino, E. "Evaluation of methods for spherical harmonic synthesis of the gravitational potential and its gradients." Advances in Space Research, Vol. 40, pp. 69–75, 2008.

[14] Casotto, S. and Fantino, E. "Gravitational gradients by tensor analysis with application to spherical coordinates." Journal of Geodesy, Vol. 83, pp. 621–634, 2009.

[15] Pavlis, N., Holmes, S., Kenyon, S., and Factor, J. "The development and evaluation of the Earth Gravitational Model 2008 (EGM2008)." Journal of Geophysical Research, Vol. 117, No. B4, 2012.

[16] Montenbruck, O. and E., G. Springer, 2012.

[17] Pollard, J. "Simplified Analysis of Low-Thrust Orbital Maneuvers." Tech. Rep. TR-2000 (8565)-10, Aerospace Corporation, El Segundo, California, 2000.